JOURNAL OF CHEMICAL & ENGINEERING DATA

ARTICLE

pubs.acs.org/jced

Thermodynamic Dissociation Constants of Butorphanol and Zolpidem by the Least-Squares Nonlinear Regression of Multiwavelength Spectrophotometric pH-Titration Data

Milan Meloun,*[,†] Zuzana Ferenčíková,[†] Martin Kaštánek,[†] and Aleš Vrána[‡]

[†]Department of Analytical Chemistry, University of Pardubice, CZ 532 10 Pardubice, Czech Republic

[‡]TEVA Czech Industries, s.r.o., CZ 747 70 Opava, Czech Republic

ABSTRACT: The mixed dissociation constants of two drugs—butorphanol and zolpidem—at temperatures of (25 and 37) °C were determined with the use of multiwavelength and multivariate treatments of spectral data using SPECFIT/32 and SQUAD(84) nonlinear regression. The factor analysis in the INDICES program predicts the correct number of components, that is, the number of dissociated and nondissociated forms of the molecules studied. The thermodynamic dissociation constant pK_a^T was estimated by nonlinear regression of $\{pK_a, I\}$ data at (25 and 37) °C: for butorphanol $pK_{a,1}^T$ = 9.46(1) and 8.99(3) and $pK_{a,2}^T$ = 9.64(2) and 9.34(3); for zolpidem $pK_{a,1}^T$ = 6.33(3) and 6.14(1), where the standard deviation in last significant digits is in parentheses. The proposed procedure involves chemical model building, calculating the concentration profiles, and fitting the protonation constants of the chemical model to multiwavelength and multivariate data measured. If the proposed protonation model represents the data adequately, the residuals should form a random pattern with a normal distribution $N(0, s^2)$, with the residual mean equal to zero, and the standard deviation of residuals being near to experimental noise. PALLAS and MARVIN predict pK_a based on the structural formulas of drug compounds in agreement with the experimental value.

INTRODUCTION

Dissociation constants are very important both in the interpretation of the mechanisms of action of drugs and in their analysis. The acid dissociation constants, pK_a, help to explain chemical phenomena such as absorption, distribution, and elimination of substances.

Butorphanol of the systematic (IUPAC) name 17-cyclobutylmethyl-morphinan-3,14-diol, CAS Registry No. 58786-99-5, ATC code N02AX02 QR05DA90, is of chemical formula $C_{21}H_{29}NO_2$ and molecular mass 327.473 g·mol^{-1}.[1] Butorphanol tartras has the structure

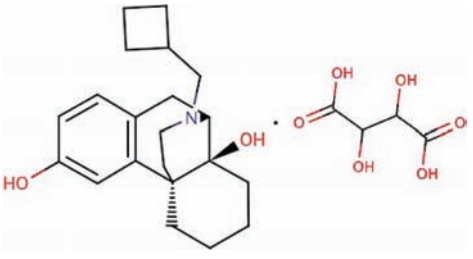

It is a morphinan-type synthetic opioid analgesic. Butorphanol being most closely structurally related to levorphanol is available only as butorphanol tartrate in injectable and intranasal spray formulations. Butorphanol exhibits partial agonist and antagonist activity at the μ opioid receptor and agonist activity at the κ opioid receptor.[2,3] Stimulation of these receptors on central nervous system neurons causes an intracellular inhibition of adenylate cyclase, closing of influx membrane calcium channels, and opening of membrane potassium channels. Butorphanol is more effective in reducing pain in women than in men.[2] In veterinary use, butorphanol is widely used as a sedative and analgesic in dogs, cats, and horses.[4]

Zolpidem of the systematic (IUPAC) name *N*,*N*,6-trimethyl-2-(4-methylphenyl)-imidazo[1,2-*a*]pyridine-3-acetamide, CAS number 82626-48-0, ATC code N05CF02 is of chemical formula $C_{19}H_{21}N_3O$ and molecular mass 307.395 g·mol^{-1}.[1] Zolpidem tartras has the structure

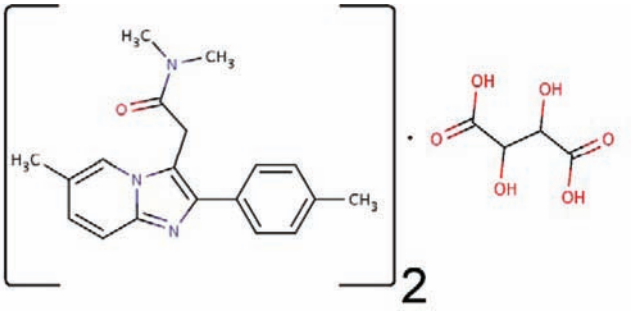

It belongs to a class of drugs called sedatives or hypnotics. Zolpidem is closely related to a family of sedatives called benzodiazepines. These drugs cause sedation and muscle relaxation, act as anticonvulsants (antiseizure), and reduce anxiety. Zolpidem has selectivity in that it has little of the muscle relaxant and antiseizure effects and more of the sedative effect. Therefore,

Special Issue: John M. Prausnitz Festschrift

Received: October 6, 2010
Accepted: January 24, 2011
Published: March 08, 2011

it is used as a medication for sleep. The oral spray form of zolpidem has more rapid absorption than the tablet form because it is absorbed through the lining of the mouth.[5] Zolpidem is a prescription medication used for the short-term treatment of insomnia, as well as some brain disorders. It is a short-acting nonbenzodiazepine hypnotic that potentiates γ-aminobutyric acid (GABA), an inhibitory neurotransmitter, by binding to γ-aminobutyric acid ($GABA_A$) receptors at the same location as benzodiazepines.[6] Its hypnotic effects are similar to those of the benzodiazepine class of drugs, but it is molecularly distinct from the classical benzodiazepine molecule and is classified as an imidazopyridine.[7,8] Because of its selective binding, zolpidem has very weak anxiolytic, myorelaxant, and anticonvulsant properties but very strong hypnotic properties.[9] Zolpidem increases slow wave sleep and caused no effect on stage 2 sleep in laboratory tests.[10]

There are several methods for the determination of dissociation constants of drugs. Traditionally, UV−vis spectrometry and potentiometry have been the most useful techniques for the determination of equilibrium constants. In addition, relevant software has been developed for the rapid theoretical estimation of pK_a values based on the chemical structure.[11,12]

Determination of the Mixed Protonation/Dissociation Constants. The procedure for the determination of the mixed protonation/dissociation constants have been described previously.[13−28] An acid−base equilibrium of the drug studied is described in terms of the protonation of the Brönstedt base L^{z-1} according to the equation $L^{z-1} + H^+ \rightleftarrows HL^z$ characterized by the thermodynamic protonation constant

$$K_H = \frac{a_{HL^z}}{a_{L^{z-1}} a_{H^+}} = \frac{[HL^z]}{[L^{z-1}][H^+]} \frac{y_{HL^z}}{y_{L^{z-1}} y_{H^+}} \quad (1)$$

The protonation equilibria between the anion L (the charges are omitted for the sake of simplicity) of a drug and a proton H are considered to form a set of variously protonated species L, LH, LH_2, LH_3, and so forth, which have the general formula L_lH_r in a particular chemical model and which are represented by n_c the number of species, r_i, $i = 1, ..., n_c$ where index i labels their particular stoichiometry; the overall protonation (stability) constant of the protonated species, β_{qr}, may then be expressed as

$$\beta_r = [LH_r]/([L][H]^r) = c/(lh^r) \quad (2)$$

where the free concentration $[L] = l$, $[H] = h$, and $[LH_r] = c$. For dissociation reactions realized at constant ionic strength the so-called, "mixed dissociation constants" are defined as

$$K_{a,j} = \frac{[H_{j-1}L] a_{H^+}}{[H_jL]} \quad (3)$$

As each aqueous species is characterized by its own spectrum, for UV−vis experiments and the ith solution measured at the jth wavelength, the Lambert−Beer law relates the absorbance, $A_{i,j}$, being defined as

$$A_{i,j} = \sum_{n=1}^{n_c} \varepsilon_{j,n} c_n = \sum_{n=1}^{p} (\varepsilon_{r,j} \beta_r l h^r)_n \quad (4)$$

where $\varepsilon_{r,j}$ is the molar absorptivity of the LH_r species with the stoichiometric coefficient r measured at the jth wavelength. The absorbance $A_{i,j}$ is an element of the absorbance matrix $\boldsymbol{A}$ of size $(n_s \cdot n_w)$ being measured for n_s solutions with known total concentrations of $n_z = 2$ basic components, c_L and c_H, at n_w wavelengths. Calculations related to the determination of protonation constants may be performed by the regression analysis of spectra using versions of the SQUAD(84) program family[13−18] and SPECFIT/32[21−24,29] and have been described previously.[30] The experimental and computational schemes for the determination of the protonation constants of the multicomponent system are taken from Meloun et al.[30]

Let us consider the dependence of the mixed dissociation constant $K_a = a_{H+}[L^{z-1}]/[HL^z]$ on an ionic strength, when both ions HL^z and L^{z-1} have roughly the same ion-size parameter $\mathring{a}$ in the dissociation equilibrium $HL^z \rightleftarrows L^{z-1} + H^+$ with the thermodynamic dissociation constant K_a^T. This dependence is expressed by the extended Debye−Hückel equation

$$pK_a = pK_a^T - \frac{A(1-2z)\sqrt{I}}{1 + B\mathring{a}\sqrt{I}} + CI \quad (5)$$

where $A = 0.5112\ mol^{-1/2} \cdot L^{1/2} \cdot K^{3/2}$ and $B = 0.3291\ mol^{-1/2} \cdot m^{-1} \cdot L^{1/2} \cdot K^{1/2}\ 10^{10}$ for aqueous solutions at 25 °C. The mixed dissociation constant pK_a represents a dependent variable, while the ionic strength I stands for the independent variable. Three unknown parameters $\boldsymbol{b} = \{pK_a, \mathring{a}\}$ are to be estimated by a minimization of the sum of the squared residuals[31]

$$U(\boldsymbol{b}) = \sum_{i=1}^{n} w_i [pK_{a,exp,i} - pK_{a,calc,i}]^2$$

$$= \sum_{i=1}^{n} w_i [pK_{a,exp,i} - f(I; pK_a^T, \mathring{a}, C]^2 = \text{minimum} \quad (6)$$

The nonlinear estimation problem is simply a problem of optimization in the parameter space, in which the pK_a and I are known and given values, while the parameters pK_a^T, $\mathring{a}$, and C are unknown variables to be estimated.[14,17,30,32,33] The adequacy of a proposed regression model with experimental data may be examined by the goodness-of-fit test, cf. a previous tutorial.[30]

Determination of the Number of Light-Absorbing Species. A qualitative interpretation of the spectra aims to evaluate of the quality of the data set and remove spurious data and to estimate the minimum number of factors, that is, contributing aqueous species, which are necessary to describe the experimental data. The INDICES[34,35] determine the number of dominant light-absorbing species present in the equilibrium mixture is based on a comparison of an actual index of method used with the experimental error of instrument used, $s_{inst}(A)$, and concerns the methods[19,34] when five of them also were used here:

(a) Kankare's residual standard deviation, $s_k(A)$. The $s_k(A)$ values for different numbers of components k are plotted against an index k, $s_k(A) = f(k)$, and the number of significant components is an integer $n_c = k$ for which $s_k(A)$ is close to the instrumental error of absorbance $s_{inst}(A)$.[19,35]

(b) Residual standard deviation, RSD(k), is used analogously as in the previous method $s_k(A)$.[19,35]

(c) Root-mean-square error, RMS: analogically as in the previous method, it is based on finding the point where the slope of the indicator function changes.[19,35]

(d) Standard deviation of eigenvalues $s(g)$ is based on finding the point where the slope of the indicator function changes.[19,35]

(e) Eigenvalues g: the first k eigenvalues being called a set of primary eigenvalues g contain contributions from the real components and should be considerably larger than those containing only noise.[19,35]

Determination of Enthalpy and Entropy Change. The enthalpy change (ΔH^0) for the dissociation process was calculated using the van't Hoff equation

$$\frac{d \ln K}{dT} = \frac{\Delta H^0}{RT^2} \quad (7)$$

From the free-energy change ΔG^0 and ΔH^0 values, the entropy (ΔS^0) could be calculated:

$$\Delta G^0 = -RT \ln K \quad (8)$$

$$\Delta S^0 = \frac{\Delta H^0 - \Delta G^0}{T} \quad (9)$$

where R (ideal gas constant) = 8.314 $J \cdot K^{-1} \cdot mol^{-1}$, K is the thermodynamic dissociation constant, and T is the absolute temperature.

EXPERIMENTAL SECTION

Chemicals. Butorphanol tartras was of content 100 % (Teva Czech Industries s.r.o. Quality Certificate SM\QC\6482796 \01), and zolpidem tartras was of content 100 %. Hydrochloric acid, 1 $mol \cdot dm^{-3}$, was prepared by diluting concentrated HCl (p.a., Lachema Brno) with redistilled water and standardization against HgO and KI with a reproducibility better than 0.2 % according to the equation $HgO + 4KI + H_2O \rightleftarrows 2KOH + K_2[HgI_4]$ and $KOH + HCl \rightleftarrows KCl + H_2O$. Potassium hydroxide, 1 $mol \cdot dm^{-3}$, was prepared from the exact weight of pellets p.a., Aldrich Chemical Co., with carbon-dioxide free redistilled water kept 50 min on the sonographic bath. The solution was stored for several days in a polyethylene bottle in argon atmosphere. This solution was standardized against a solution of potassium hydrogen phthalate using the derivative method with a reproducibility of 0.1 %. Mercury oxide, potassium iodide, and potassium chloride, p.a. Lachema Brno, were not extra purified. Twice-redistilled water kept 50 min on the sonographic bath was used in the preparation of solutions. The preparation of other solutions from analytical reagent-grade chemicals has been described previously.[23]

pH Spectrophotometric Titration Procedure. The apparatus Cintra 40 (GBC, Australia) spectrophotometer used and the pH-spectrophotometric titration procedure have been described previously.[30] An experimental and computational scheme for the protonation model building of a multicomponent and multiwavelength system was proposed by Meloun et al., cf. page 226 in ref 36 or refs 15 and 30, and is here revised with regard to SPECFIT/32, SQUAD(84), and INDICES applications. When a minimization process terminates, some diagnostics are examined to determine whether the results should be accepted. The physical meaning of parametric estimates:

(1) Instrumental error of absorbance measurements, $s_{inst}(A)$: The INDICES algorithm cf. ref 34 should be used to evaluate $s_{inst}(A)$. This value can be used for prediction of the signal-to-error ratio, SER, for experimental data. It was proven that the indices are able to accurately predict the correct number of components that contribute to a set of absorption spectra for data sets with SER being equal to or higher than 10.

(2) Experimental design: Simultaneous monitoring of absorbance and pH during titrations is used in a titration.

(3) Number of light-absorbing species: The INDICES[34] can detect minor components and predicts the correct number of components for data sets with the SER of at least equal to or higher than 10. For the signal value S in a numerator of the ratio S/E, the absorbance difference for the jth-wavelength at the ith-spectrum $\Delta_{ij} = A_{ij} - A_{i,acid}$ can be used, where $A_{i,acid}$ is the limiting spectrum of acid form of drug measured. This absorbance change Δ_{ij} is then divided with the instrumental standard deviation $s_{inst}(A)$ and resulting ratio $\Delta/s_{inst}(A)$ represents here the SER of spectra studied.

(4) Choice of computational strategy: The input data should specify whether β_{qr} or log β_{qr} values are to be refined whether multiple regression (MR) or non-negative linear least-squares (NNLS) are desired.[13,15]

(5) Theoretically predicted parameter β_{qr} estimates: Two predicting programs, PALLAS[11] and MARVIN,[37] provide a collection of powerful tools for making a prediction of the pK_a values of any organic compound on the basis of base on the structural formulas of the compounds, using approximately 300 Hammett and Taft equations. Ab initio quantum mechanics calculations have been used extensively, as have semiempirical quantum mechanics.[38]

(6) Diagnostics indicating a true chemical model: When the minimization process of a regression spectra analysis terminates, some diagnostic criteria are examined to determine whether the results should be accepted or rejected.

First diagnostic—the physical meaning of the parametric estimates: The physical meaning of the protonation constants, associated molar absorptivities, and stoichiometric indices is examined: β_{qr} and ε_{qr} should be neither too high nor too low, and ε_{qr} should not be negative. The absolute values of $s(\beta_j)$, $s(\varepsilon_j)$ give information about the last RSS-contour of the hyperparaboloid in neighborhood of the pit, RSS_{min}.

Second diagnostic—the physical meaning of the species concentrations: There are some physical constraints which are generally applied to realistic concentrations of species and also their molar absorptivities: concentrations and molar absorptivities must be positive numbers.

Third diagnostic—parametric correlation coefficients: Two completely correlated species cannot be included in a chemical model, because the relevant protonation constants are strongly correlated and an increase or decrease of one component may compensated for the other.

Fourth diagnostic—goodness-of-fit test: The goodness-of-fit achieved is easily seen by examination of the differences between the experimental and the calculated values of absorbance, $e_i = A_{exp,i,j} - A_{calc,i,j}$. One of the most important statistics calculated is the standard deviation of the absorbance, $s(A)$, calculated at the termination of the minimization process as $s(A) = (U_{min}/df)^{1/2}$ where U_{min} stands for the residuals-square-sum function in minimum and df is the degree of freedom. This is usually compared with the standard deviation of absorbance calculated by the INDICES program[34] $s_k(A)$ and the instrumental error of

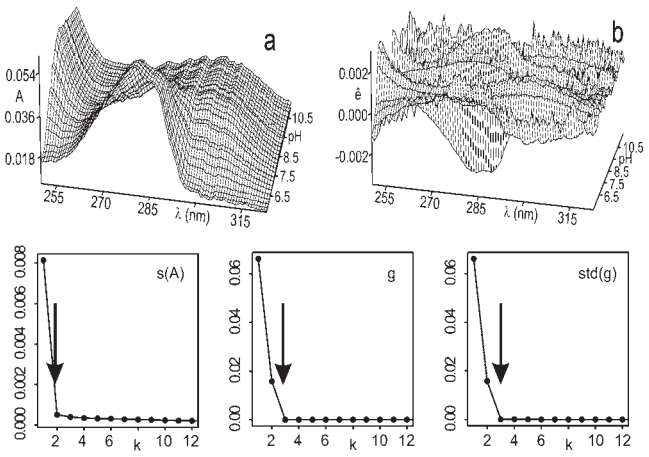

Figure 1. Upper row graphs: (a) The 3D absorbance−response surface representing the measured multiwavelength absorption spectra for $2.48 \cdot 10^{-5}$ M butorphanol in dependence on pH at 25 °C and I = 0.022 (KCl), (b) the 3D residuals map after nonlinear regression performed with SPECFIT and SQUAD (S-Plus). Low row graphs: The Cattel's index plot of eigenvalues in form of indices modifying methods as a function of the number of principal components k for the pH−absorbance matrix from Figure 1a. Left: Kankare's residual standard deviation, $s_k(A)$. Middle: Standard deviation of eigenvalues $s(g)$. Right: Eigenvalues (g). The arrows indicate that most of methods lead to two or three light-absorbing species in pH-equilibrium mixture (S-Plus).

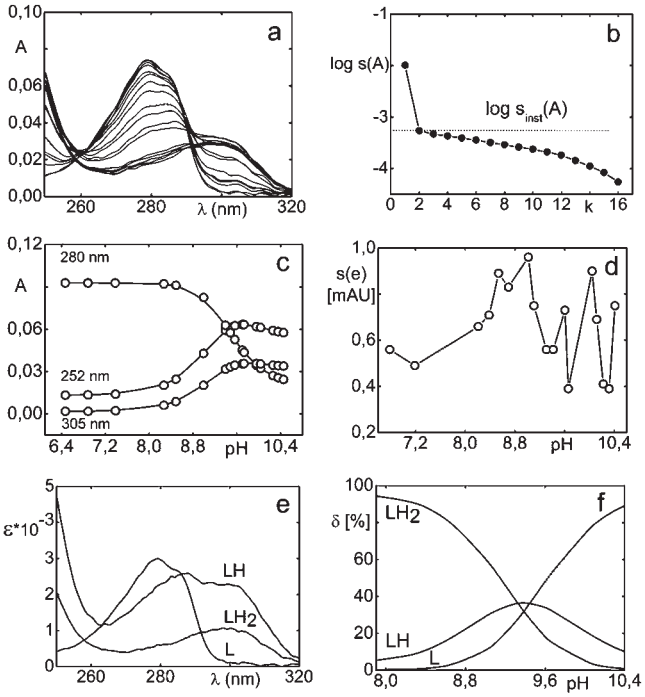

Figure 2. Nonlinear regression analysis of the protonation equilibria model and factor analysis of $2.48 \cdot 10^{-5}$ M butorphanol in dependence on pH at 25 °C and I = 0.022 (KCl): (a) the 2D absorption spectra in dependence on pH at 25 °C; (b) the Cattel's scree plot of the Wernimont−Kankare procedure for the determination of the number of light-absorbing species in the mixture k^* = 2 leading to the actual instrumental error of the spectrophotometer used $s_{inst}(A)$ = 0.55 mAU (INDICES in S-Plus); (c) the scatterplot of absorbance vs. pH curves for (252, 280, and 305) nm at 25 °C proves an existence of protonation equilibrium of butorphanol; (d) the scatterplot of residuals expressed with the standard deviation of individual spectra in dependence on pH; (e) the pure spectra profiles of molar absorptivities vs wavelengths for species L and LH; (f) the distribution diagram of the relative concentrations of species L and LH in dependence on pH at 25 °C. The charges of species are omitted for the sake of simplicity (SPECFIT, ORIGIN).

the spectrophotometer used $s_{inst}(A)$, and if it is valid that $s(A) \leq s_k(A)$, or $s(A) \leq s_{inst}(A)$, then the fit is considered to be statistically acceptable. Alternatively, the statistical measures of residuals $\boldsymbol{e}$ can be calculated to examine the following statistical criteria: the residual bias $\bar{e}$ should be a value close to zero; the residual standard deviation $s(e)$ being equal to the absorbance standard deviation $s(A)$ should be close to the instrumental standard deviation $s_{inst}(A)$. The residual skewness $g_1(e)$ should be close to zero for a symmetric distribution of residuals; the residual kurtosis $g_2(e)$ should be close to 3 for a Gaussian distribution of residuals.

Fifth diagnostic—deconvolution of spectra: Resolution of each experimental spectrum into spectra of the individual species proves whether the experimental design has been proposed to be efficient enough. If the model represents the data adequately, the residuals should possess characteristics that agree with, or at least do not refute, the basic sample assumptions: the residuals should be randomly distributed about the A_{calc} values predicted by the regression equation. Systematic departures from randomness indicate that the model is not satisfactory. Examination of plots of the residuals versus λ may assist numerical and/or graphical aids in the analysis of residuals.

Reliability of the Estimated Protonation Constants. The adequacy of a proposed regression model with experimental spectra and the reliability of parameter estimates $\beta_{qr,j}$ found (being denoted for the sake of simplicity here as b_j (j = 1, ..., m) and ε_{ij} (j = 1, ..., n_w) may be examined by a goodness-of-fit test, cf. page 101 in ref 36:

(1) The quality of parameter estimates b_j (j = 1, ..., m) found is reviewed according to the variances $D(b_j)$. Often an empirical rule is used: parameter b_j differs significantly from zero when its estimate is greater than 3 standard deviations, $3[D(\hat{e})]^{1/2} \leq |b_j|$ (j = 1, ..., m).

(2) The quality of the experimental data is examined by identification of the influential points (namely outliers) with the use of regression diagnostics, cf. page 62 in ref 33.

(3) The quality of curve fit achieved: the adequacy of the proposed model and m parameter estimates found with n values of experimental data is examined by a goodness-of-fit test based on the statistical analysis of classical residuals. Examination of residual plots may be assisted by graphical analysis of the residuals, cf. pages 289 and 290 in ref 33.

Computation. Computation relating to the determination of dissociation constants were performed by regression analysis of the UV−vis spectra using the SQUAD(84)[15] and SPECFIT/32[21−24,29] programs. Most of graphs were plotted using ORIGIN 7.5[39] and S-Plus.[40] The thermodynamic dissociation constant pK_a^T was estimated with the MINOPT nonlinear regression program in the ADSTAT statistical system (TriloByte Statistical Software, Ltd., Czech Republic).[41] A qualitative interpretation of the spectra with the use of the INDICES program[34] aims to evaluate the quality of the data set and remove spurious data and to estimate the minimum number of factors, that is, contributing aqueous species, which are necessary to describe the experimental data and determine the number of dominant

Table 1. Dependence of the Mixed Dissociation Constants pK_a of Butorphanol on Ionic Strength Using Regression Analysis of pH-Spectrophotometric Data with SPECFIT at 25 °C and 37 °C[a]

25 °C							
ionic strength		0.0228	0.0418	0.0673	0.0895	0.1118	0.0134
SPECFIT	pK_{a1}	9.320(40)	9.282(40)	9.262(30)	9.256(40)	9.242(30)	9.224(30)
	$s(A)$ [mAU]	0.56	0.50	0.52	0.50	0.73	0.48
	pK_{a2}	9.454(50)	9.387(40)	9.398(30)	9.325(40)	9.298(50)	9.284(30)
	$s(A)$ [mAU]	0.56	0.50	0.52	0.50	0.73	0.48
SQUAD	pK_{a1}	9.322(20)	9.278(20)	9.265(10)	9.261(10)	9.246(20)	9.166(10)
	$s(A)$ [mAU]	0.73	0.66	0.36	0.61	0.82	0.62
	pK_{a2}	9.447(20)	9.386(10)	9.394(10)	9.307(10)	9.296(20)	9.284(10)
	$s(A)$ [mAU]	0.73	0.66	0.70	0.61	0.82	0.62
37 °C							
ionic strength		0.0228	0.0418	0.0895	0.1118	0.1339	0.1562
SPECFIT	pK_{a1}	8.756(40)	8.652(41)	8.617(33)	8.577(30)	8.485(34)	8.501(70)
	$s(A)$ [mAU]	0.25	0.54	0.37	0.28	0.54	0.35
	pK_{a2}	9.098(60)	9.018(65)	8.852(66)	8.806(40)	8.754(76)	8.623(30)
	$s(A)$ [mAU]	0.25	0.54	0.37	0.28	0.54	0.35
SQUAD	pK_{a1}	8.782(30)	8.669(18)	8.676(15)	8.571(10)	8.482(14)	8.509(30)
	$s(A)$ [mAU]	0.45	0.76	0.57	0.43	0.72	0.51
	pK_{a2}	9.087(30)	9.014(21)	8.805(28)	8.814(20)	8.755(27)	8.614(10)
	$s(A)$ [mAU]	0.45	0.76	0.57	0.43	0.72	0.51

[a] The standard deviations of the parameter pK_a in the last valid digits are in parentheses.

species present in the equilibrium mixture. PALLAS[11] and MARVIN[37] are programs for making predictions based on the structural formulas of drug compounds.

Input Data Available on Web. Complete experimental and computational procedures, input data specimens, and corresponding output in numerical and graphical form for three programs, INDICES, SQUAD(84), and SPECFIT/32, are available free of charge online at http://meloun.upce.cz and in the block DOWNLOAD and DATA.

RESULTS AND DISCUSSION

Butorphanol and zolpidem which were studied in our laboratory represent two drugs which exhibit some small changes in spectra. Other instrumental methods could not be used for limited solubility in water.

Butorphanol. A suggested strategy for an effective experimentation in dissociation constants determination ensued from spectral data treatment is presented on the protonation equilibria of butorphanol. The 16 experimental spectra at various pH values at 35 wavelengths are acquired for the titration of $2.48 \cdot 10^{-5}$ M butorphanol solution by a standard solution of 1 M KOH to adjust the pH value at 25 °C and I = 0.022 (KCl). As all variously protonated anions exhibit quite similar absorption bands, a part of spectrum from (250 to 320) nm was selected as the most appropriate for an estimation of protonation constants. The pH-spectrophotometric titration allows absorbance−response surface data (Figures 1a and 2a) to be acquired for analysis with nonlinear regression, and the reliability of parameter estimates (pK_a^T and ε'_s) can be assessed on the basis of the goodness-of-fit test of residuals (Figures 1b and 2d). The adjustment of pH value from 6 to 11 causes the absorbance to change by 0.080 of the A−pH curve only (Figure 2c), so that the monitoring of three components L^{2-}, HL^-, and H_2L of the protonation equilibrium is rather unsure. As the changes in spectra are small, a very precise measurement of absorbance is necessary for a reliable detection of the deprotonation equilibrium studied. In the first step of the regression spectra analysis, the number of light-absorbing species was estimated using the INDICES algorithm (Figures 1 and 2b). The number of light-absorbing species p can be predicted from the index function values by finding the point $p = k$ where the slope of index function $PC(k) = f(k)$ changes or by comparing $PC(k)$ values to the instrumental error $s_{inst}(A)$. This is the common criterion for determining p (lower part of Figure 1). A very low value of $s_{inst}(A)$ in Figure 2b proves that a sufficiently precise spectrophotometer and efficient experimental technique were used. The position of the break point on the $s_k(A) = f(k)$ curve in the factor analysis scree plot in Figure 2b gives k = 2 with the corresponding coordinate $s_2(A)$ = 0.55 mAU (i.e., $\log s_2(A) = -3.26$) which may also be taken as the actual instrumental error $s_{inst}(A)$ of the spectrophotometer used. While the first Kankare method (denoted in Figure 1 as $s(A)$) estimates two species only, the other two methods of modified factor analysis on the lower part of Figure 1 estimate three light-absorbing components L^{2-}, HL^-, and H_2L of the protonation equilibrium. The absorbance−pH curves at three selected wavelengths (Figure 2c) have proven that the protonation equilibria significantly affect the chromophore in the butorphanol molecule, but both variously protonated species LH_2 and LH^- exhibit similar absorption bands. In the first run, the both dissociation constants pK_{a1} and pK_{a2} and molar absorptivities of butorphanol by SPECFIT/32 are estimated. The goodness-of-fit of spectra calculated and following graphical analysis of residuals (Figure 2d) establishes sufficiently reliable estimates of the two dissociation constants and three molar absorption coefficients. The estimated mixed dissociation constants pK_{a1} and pK_{a2} at two temperatures (25 and 37) °C in dependence on an ionic strength I are in Table 1.

Table 2. Search for a Protonation Model of Butorphanol with SQUAD(84) Analysis of A−pH spectra at 25 °C and Ionic Strength I = 0.001[a]

	first hypothesis	second hypothesis
model hypothesis	L, LH	L, LH, LH_2
k, $s_k(A)$ [mAU]	2, 0.52	3, 0.39
pK_{a1}	9.151(21)	9.201(19)
pK_{a2}		9.583(19)
$s(A)$ [mAU]	2.70	0.64
$s(e)$ [mAU]	2.70	0.64
|| [mAU]	2.00	0.40
$g_1(e)$	−0.0566	0.4309
$g_2(e)$	3.74	3.49
R-factor [%]	8.99	2.07
model is	rejected	accepted

[a] The standard deviations in the last valid digits are in parentheses.

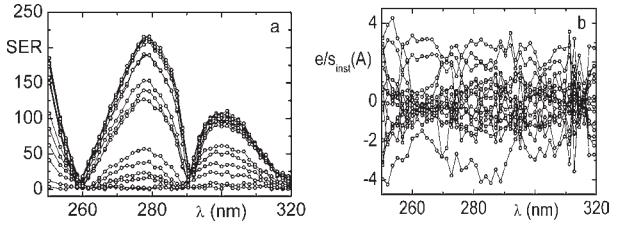

Figure 3. (a) Plot of small absorbance changes in the spectrum of butorphanol means that the value of the absorbance difference for the jth-wavelength of the ith-spectrum $\Delta_{ij} = A_{ij} - A_{i,acid}$ is divided by the instrumental standard deviation $s_{inst}(A)$, and the resulting ratios SER = $\Delta/s_{inst}(A)$ are plotted in dependence of wavelength λ for all absorbance matrix elements, where $A_{i,acid}$ is the limiting spectrum of the acid form of the drug measured. This ratio is compared with the limiting SER value for the methotrexate to test if the absorbance changes are significantly larger than the instrumental noise. (b) The plot of the ratio $e/s_{inst}(A)$, that is, the ratio of the residuals divided by the instrumental standard deviation $s_{inst}(A)$ in dependence on wavelength λ for all of the residual matrix elements for butorphanol tests if the residuals are of the same magnitude as the instrumental noise.

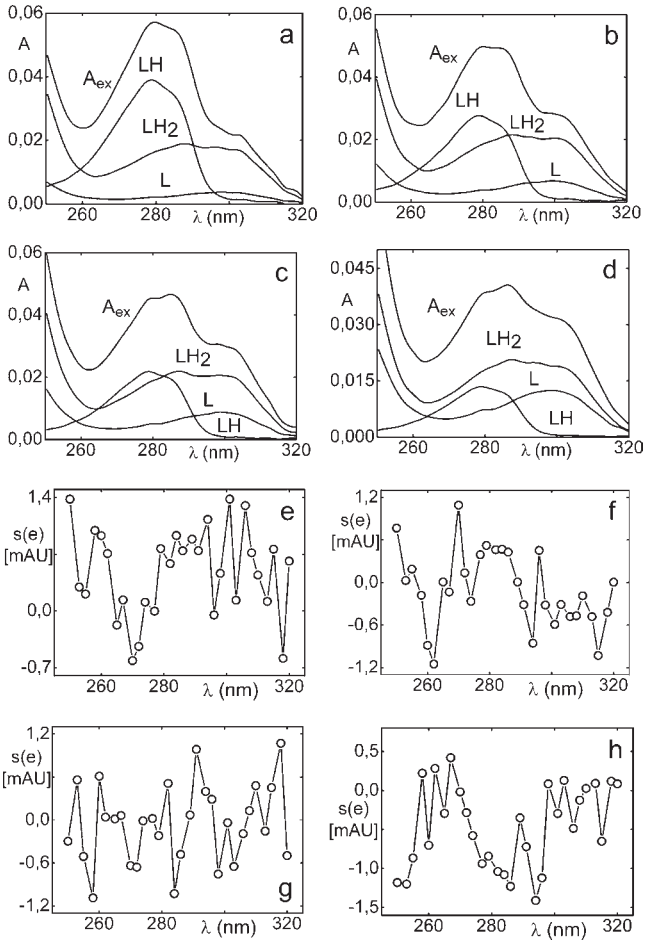

Figure 4. (a, b, c, d) Spectra deconvolution of butorphanol from Figure 1a into spectra of the individual species for four important values of pH, proving that the experimental design is efficient enough. (e, f, g, h) No systematic departures from randomness in residuals, proving that the model proposed is satisfactory.

The reliability of the dissociation constants estimates found may be tested using the following diagnostics.

The first diagnostic indicates whether all of the estimates $pK_{a,r}$ and ε_r have physical meaning and reach realistic values for 16 values of pH spectra of butorphanol measured at 35 wavelengths. As the standard deviations $s(pK_a)$ of parameters pK_a and $s(\varepsilon_r)$ of parameters ε_r are significantly smaller than their corresponding parameter estimates (Table 1), all variously protonated species are statistically significant at a significance level α = 0.05. As the two protonation models in the model search of Table 2 (first model: L, HL, second model: L, HL, H_2L) were tested, it may be concluded that regression spectra analysis can distinguish among these two models, and on the basis of a very good spectra fitting, the model L, HL, H_2L was proven.

The second diagnostic tests whether all of the calculated free concentrations of the three variously protonated species on the distribution diagram of the relative concentration expressed as a percentage have physical meaning, which proved to be the case. The calculated free concentration of the basic components and variously protonated species of the protonation equilibria model should show molarities higher than 10^{-8} M. As the numerical values of protonation/dissociation constants and molar absorption coefficients may not seem very interesting, a graphical representation (Figure 2e,f) is more illustrative, and graphs also form efficient diagnostic tools in the search for the most probable chemical model. A distribution diagram of relative concentration shows the protonation equilibria of L, HL, and H_2L in dependence on pH in Figure 2f and makes it easier to judge the contributions of individual species to the total concentration quickly.

The third diagnostic concerning the matrix of correlation coefficients in output of SQUAD(84) proves that there is an interdependence of two pairs of protonation constants of butorphanol $r(\log \beta_{11}$ vs $\log \beta_{12}) = 0.7910$ which indicate that their estimation will be more difficult.

The fourth diagnostic concerns the goodness-of-fit. It is easily seen by examination of the differences between the experimental and the calculated values of absorbance, $e_i = A_{exp,i,j} - A_{calc\ i,j}$. Examination of the spectra and of the graph of the predicted absorbance−response surface through all experimental points (Figures 1b and 2d) should reveal whether the results calculated are consistent and whether any gross experimental errors have been made in the measurement of the spectra. One of the most important statistics calculated is the standard deviation of

Table 3. Thermodynamic Dissociation Constants pK_a^T for Butorphanol at Two Temperatures 25 °C and 37 °C[a]

		estimated in this work			
		SPECFIT		SQUAD	
	predicted PALLAS, MARVIN	25 °C	37 °C	25 °C	37 °C
pK^T_{a1}		9.465(9)	8.991(32)	9.465(15)	9.009(57)
pK^T_{a2}	10.38, 10.70	9.642(22)	9.344(32)	9.634(23)	9.328(32)

[a] The standard deviations in the last valid digits are in parentheses.

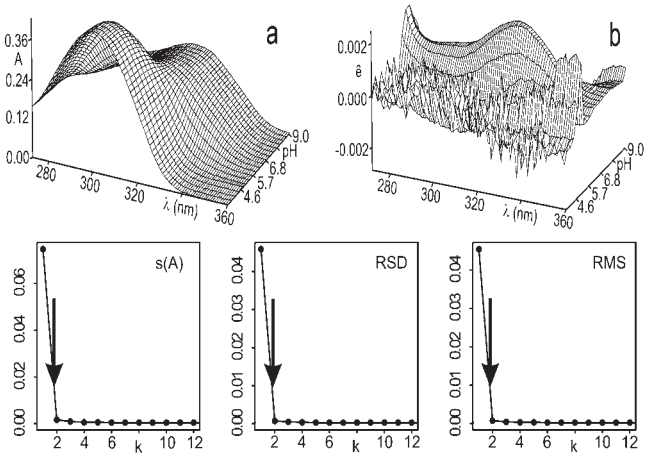

Figure 5. Upper row graphs: (a) the 3D absorbance−response surface representing the measured multiwavelength absorption spectra for $3.38 \cdot 10^{-5}$ M zolpidem in dependence on pH at 25 °C and I = 0.006 (KCl), (b) the 3D residuals map after nonlinear regression performed with SPECFIT and SQUAD (S-Plus). Low row graphs contain the Cattel's index plot of eigenvalues in form of indices modifying methods as a function of the number of principal components k for the pH−absorbance matrix from Figure 4a. Left: Kankare's residual standard deviation, $s_k(A)$. Middle: The residual standard deviation RSD(k). Right: The root-mean-square error RMS(k). The arrows indicate that most of methods lead to two light-absorbing species in pH-equilibrium mixture (S-Plus).

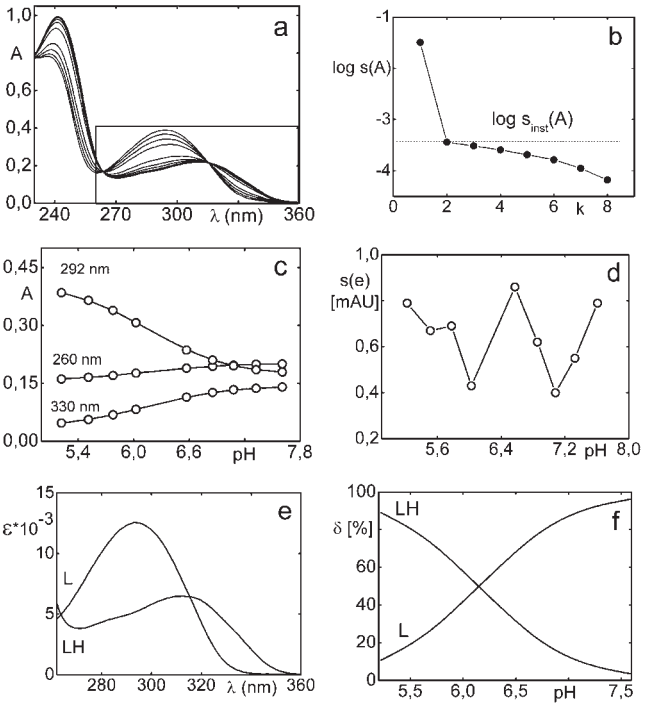

Figure 6. Nonlinear regression analysis of the protonation equilibria model and factor analysis of $3.38 \cdot 10^{-5}$ M zolpidem in dependence on pH at 25 °C and I = 0.006 (KCl): (a) the 2D absorption spectra in dependence on pH at 25 °C; (b) the Cattel's scree plot of the Wernimont−Kankare procedure for the determination of the number of light-absorbing species in the mixture k^* = 2 leading to the actual instrumental error of the spectrophotometer used $s_{inst}(A)$ = 0.36 mAU (INDICES in S-Plus); (c) the absorbance vs pH curves for (260, 292, and 330) nm at 25 °C; (d) the scatter plot of residuals expressed with the standard deviation of individual spectra in dependence on pH; (e) the pure spectra profiles of molar absorptivities vs wavelengths for species L and LH; (f) the distribution diagram of the relative concentrations of species L and LH in dependence on pH at 25 °C. The charges of species are omitted for the sake of simplicity (SPECFIT, ORIGIN).

absorbance, $s(A)$, calculated from a set of refined parameters at the termination of the minimization process. This is usually compared to the standard deviation of absorbance calculated by the INDICES program, $s_k(A)$, and if $s(A) \leq s_k(A)$ or $s(A) \leq s_{inst}(A)$, the instrumental error of the spectrophotometer used, the fit is considered to be statistically acceptable (Table 2). This proves that the $s_2(A)$ value is equal to 0.52 mAU or $s_3(A)$ value is equal to 0.39 mAU and is close to the standard deviation of absorbance when the minimization process of SPECFIT terminates, $s(A)$ = 0.35 mAU. Although this statistical analysis of residuals gives the most rigorous test of the degree-of-fit, realistic empirical limits must be used. The statistical measures of all residuals e prove that the minimum of the eliptic hyperparaboloid U is reached with SQUAD(84): the residual standard deviation $s(e)$ = 0.64 mAU always has sufficiently low values. The graphical presentation of the residuals in Figure 1b and 5b assists the detection of an outlier spectrum point, a trend in the spectrum residuals, or an abrupt shift of level in the spectra. The statistical measures of all of the residuals from Figure 1b prove that the minimum of the eliptic hyperparaboloid is reached: the mean residual $|\bar{e}|$ = 0.40 mAU and the residual standard deviation $s(e)$ = 0.64 mAU have sufficiently low values. The skewness $g_1(e)$ = 0.43 is close to zero and proves a symmetric distribution of the residuals set, while the kurtosis $g_2(e)$ = 3.49 is close to 3 proving a Gaussian distribution. The Hamilton R-factor of relative fitness is 2.07 % calculated with SQUAD(84) only, proving so an excellent achieved fitness, and the parameter estimates may therefore be considered reliable.

To express and analyze small changes of absorbance in the spectral set, the absorbance differences for the jth wavelength of the ith spectrum $\Delta_i = A_{ij} - A_{i,acid}$ were calculated so that from the absorbance value of the spectrum measured at the actual pH the absorbance value of the acidic form was subtracted. The absorbance difference Δ_i was then divided by the actual instrumental

Table 4. Dependence of the Mixed Dissociation Constants pK_a of Zolpidem on Ionic Strength Using Regression Analysis of pH-Spectrophotometric Data with SPECFIT at 25 °C and 37 °C[a]

25 °C							
ionic strength		0.0061	0.0294	0.0418	0.0673	0.0895	0.1117
SPECFIT	pK_a	6.329(7)	6.343(8)	6.370(4)	6.389(6)	6.403(4)	6.423(4)
	$s(A)$ [mAU]	0.79	0.86	0.72	0.77	0.63	0.72
SQUAD	pK_a	6.330(2)	6.344(2)	6.370(1)	6.389(2)	6.403(1)	6.423(2)
	$s(A)$ [mAU]	0.97	0.96	0.83	0.85	0.68	1.05
37 °C							
ionic strength		0.0061	0.0294	0.0418	0.0673	0.0895	0.1117
SPECFIT	pK_a	6.142(8)	6.163(8)	6.166(4)	6.193(6)	6.208(7)	6.224(7)
	$s(A)$ [mAU]	0.59	0.82	0.4	0.62	0.74	0.53
SQUAD	pK_a	6.140(3)	6.163(2)	6.166(2)	6.193(2)	6.208(2)	6.229(3)
	$s(A)$ [mAU]	0.74	0.10	0.56	0.75	0.90	0.57

[a] The standard deviations of the parameter pK_a in the last valid digits are in parentheses.

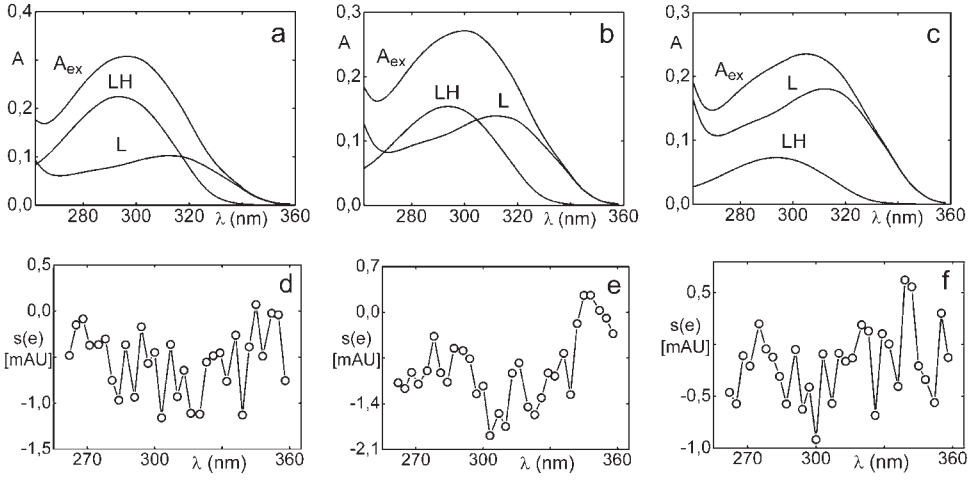

Figure 7. (a, b, c) Spectra deconvolution of zolpidem from Figure 4a into spectra of the individual species for four important values of pH, proving that the experimental design is efficient enough. (d, e, f) No systematic departures from randomness in residuals, proving that the model proposed is satisfactory.

standard deviation $s_{inst}(A)$ of the spectrophotometer used, and the resulting value represents the SER value. Figure 3a shows a graph of the SER in dependence on wavelength in the measured range for drug used. When the SER is larger than 10, a factor analysis is sufficiently able to predict the correct number of light-absorbing components in the equilibrium mixture. To prove that nonlinear regression also can analyze such data of small absorbance changes, the residuals set was compared with the instrumental noise $s_{inst}(A)$. If the ratio $e/s_{inst}(A)$ is of similar magnitude, that is, nearly equal to one, it means that sufficient curve fitting was achieved by the nonlinear regression of the spectra set and that the minimization process found the minimum of the residual-square-sum function U_{min}. Figure 3b shows a comparison of the ratio $e/s_{inst}(A)$ in dependence on wavelength for butorphanol measured. From the figure it is obvious that most of the residuals are of the same magnitude as the instrumental noise and so proves a sufficient reliability of the regression process performed.

The fifth diagnostic, the spectra deconvolution in Figures 4 and 7, shows the deconvolution of the experimental spectrum into spectra of the individual variously protonated species to examine whether the experimental design is efficient. In spectrophotometry a plot of the experimental absorbance curve and a calculated absorbance curve for each individual species in the mixture (Figure 3) is often used. As the additivity of absorbance should be proven, the sum of all of the absorbances of the variously protonated species at a given wavelength should be equal to the experimental absorbance. The resolution of each experimental spectrum of butarphanol into spectra of the individual species proves the experimental design of a pH-spectrophotometric titration which has been proposed to be efficient enough (Figure 4a,b,c,d) and analogically for zolpidem (Figure 7). If, for a particular pH range, the spectrum consists of just a single component, further spectra for that range would be redundant, although they could improve the precision. In pH ranges where more components contribute significantly to the spectrum, several spectra should be measured. Such a spectrum provides sufficient information for a regression analysis which monitors at least two species in equilibrium where none of them is a minor species. The minor species has a relative concentration in a distribution diagram of less than 5 % of the total concentration of the basic

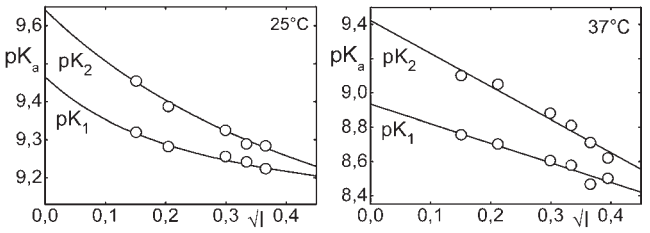

Figure 8. Dependence of the mixed dissociation constant pK_a of butorphanol on the square root of the ionic strength, leading to the thermodynamic dissociation constant; $pK^T_{a,1}$ = 9.46(1) and 8.99(3) and $pK^T_{a,2}$ = 9.64(2) and 9.34(3) at (25 and 37) °C (ADSTAT, ORIGIN).

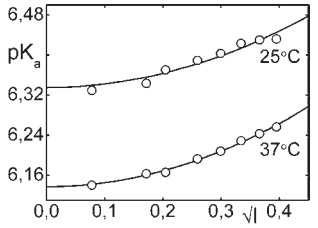

Figure 9. Dependence of the mixed dissociation constant pK_a of zolpidem on the square root of the ionic strength, leading to the thermodynamic dissociation constant; $pK^T_{a,1}$ = 6.33(3) and 6.14(1) at (25 and 37) °C (ADSTAT, ORIGIN).

component c_L. When, on the other hand, only one species prevails in solution, the spectrum yields quite poor information for a regression analysis, and the parameter estimate is rather unsure and definitely not reliable enough. Spectrum deconvolution seems to be quite an useful tool in the proposal of an efficient experimentation strategy. As the protonation model proposed represents here the data adequately, there are no systematic departures from randomness in residuals. Table 1 shows that the standard deviation of absorbance $s(A)$ for an every set of pH absorbance matrix reached very low value being quite close to the instrumental error of spectrophotometer used, $s_{inst}(A)$, that is, about 0.35 mAU. The graphical presentation of the residuals in Figure 4e,f,g,h is of great help in the diagnostic of the rigorous statistical analysis of residuals detecting, from example, no outliers in spectra, no trend in the residuals, sufficiently frequent changes of a sign of residuals, no detection of any abrupt shift of level in the spectrum, and proving a symmetry in the residuals distribution.

Applying a Debye−Hückel equation to the data of Table 1 according to the regression criterion (eq 6), the unknown parameter pK^T_a has been estimated. Table 3 brings point estimates of the thermodynamic dissociation constants of butorphanol studied at two temperatures. Because of the narrow range of ionic strength the ion-size parameter $\mathring{a}$ and the salting-out coefficient C could not be estimated here.

Thermodynamic parameters ΔH^0 and ΔG^0 have been determined from the temperature variation of dissociation constants using van't Hoff's equation. The values of enthalpy $\Delta H^0(pK_{a1})$ = 63.9 kJ·mol^{-1} shows the dissociation process is endothermic. Positive values of ΔG^0 = 54.0 kJ·mol^{-1} at 25 °C and ΔG^0 = 55.0 kJ·mol^{-1} at 37 °C indicate that the dissociation process is not spontaneous.

Zolpidem. The experimental spectra are acquired for the titration of an acid in $3.38 \cdot 10^{-5}$ M zolpidem solution by a standard solution of 1 M KOH to adjust pH value at 25 °C and I = 0.006 (KCl). The pH spectrophotometric titration allows absorbance−response data (Figure 5) to be acquired for analysis with nonlinear regression, and the reliability of parameter estimates (pK'_s and ε'_s) can be assessed on the basis of the goodness-of-fit test of residuals (Figure 6b). As the changes in absorbance spectra are significant within deprotonation, both of the variously protonated species L^- and LH exhibit sufficiently different absorption bands. The best region of the spectrum seems to be (260 to 360) nm. In the first step of the regression spectra analysis the number of light-absorbing species is estimated by the INDICES algorithm (Figures 5 and 6b). The position of the break point on the $s_k(A) = f(k)$ curve in the factor analysis scree plot in Figure 5b is calculated and gives k^* = 2 with corresponding coordinate $\log(s_2^*(A))$ = −3.44 which gives the value $s_2^*(A)$ = 0.36 mAU. The goodness-of-fit establishes sufficiently reliable estimates of the dissociation constant and molar absorption coefficient. Figure 6e shows the curves of molar absorption coefficients of L^- and LH species in dependence on wavelength and Figure 6f the distribution diagram of L^- and LH species in dependence on pH. The estimated dissociation constant pK_a at two temperatures (25 and 37) °C in dependence on an ionic strength I is in Table 4.

The thermodynamic dissociation constants as the unknown parameter pK^T_a was estimated by applying a Debye−Hückel equation to the data in Tables 3 and 4 and Figures 8 and 9 according to the regression criterion; Tables 3 and 5 show point estimates of the thermodynamic dissociation constants of the two drugs, butorphanol and zolpidem, at two temperatures. Because of the narrow range of ionic strengths the ion-size parameter $\mathring{a}$ and the salting-out coefficient C could not be estimated.

Thermodynamic parameters ΔH^0, ΔG^0, and ΔS^0 have been determined from the temperature variation of dissociation constants using van't Hoff's equation. The values of enthalpy ΔH^0-(pK_{a1}) = 29.2 kJ·mol^{-1} show that the dissociation process is endothermic. Positive values of ΔG^0 = 36.1 kJ·mol^{-1} at 25 °C and ΔG^0 =36.4 kJ·mol^{-1} at 37 °C indicate that the dissociation process is not spontaneous, which was confirmed by a negative value of entropy ΔS^0 = −23.3 J·mol^{-1}.

Table 5. Thermodynamic Dissociation Constants pK^T_a for Zolpidem at Two Temperatures 25 °C and 37 °C[a]

		estimated in this work			
	predicted	SPECFIT		SQUAD	
	PALLAS, MARVIN	25 °C	37 °C	25 °C	37 °C
pK^T_a	6.35	6.335(27)	6.137(10)	6.333(32)	6.137(41)

[a] The standard deviations in the last valid digits are in parentheses.

LITERATURE COMPARISON

It is wise before starting a regression to analyze actual experimental data, to search for scientific library sources to obtain a good default for the number of ionizing groups, and numerical values for the initial guess as to relevant stability (protonation) constants and the probable spectral traces of all the expected components. The programs PALLAS[11] and MARVIN[37] provide a collection of powerful tools for making a prediction of the pK_a values of any organic compound on the basis of base on the structural formulas of the compounds, using approximately 300 Hammett and Taft equations. Depending on the nature of the chemical structure and based on the hypothesis

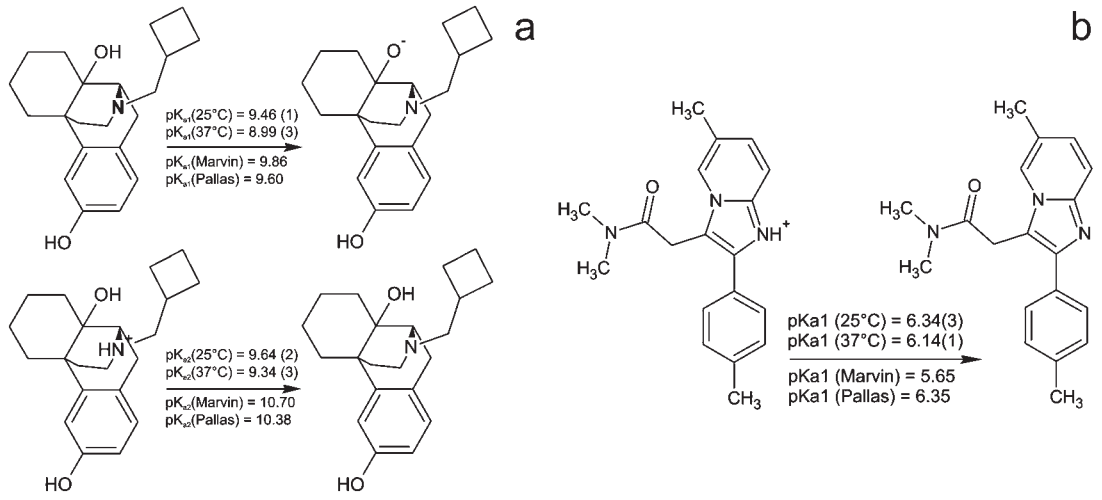

Figure 10. Protonation schema of (a) butorphanol and (b) zolpidem.

that the ionization state of a particular group is dependent upon its subenvironments constituted by its neighboring atoms and bonds, a hierarchical tree is constructed from the ionizing atom outward. Predicted values of two dissociation constants for butorphanol are $pK_{a1,pred}$ = 9.60 and $pK_{a2,pred}$ = 10.38 and for zolpidem $pK_{a1,pred}$ = 6.37. An agreement with values found in literature shows protonation schema in Figure 10 and in Table 3 and 5.

CONCLUSIONS

When drugs are very poorly soluble, pH-spectrophotometric titration may be used with nonlinear regression of the absorbance−response surface data instead of performing a potentiometric determination of the dissociation constants. The reliability of the dissociation constants of the two drugs, butorphanol and zolpidem, may be proven with goodness-of-fit tests of the absorption spectra measured at various pH values. The dissociation constant pK_a was estimated by nonlinear regression of {pK_a, I} data at (25 and 37) °C: for butorphanol $pK^T_{a,1}$ = 9.46(1) and 8.99(3) and $pK^T_{a,2}$ = 9.64(2) and 9.34(3); for zolpidem $pK^T_{a,1}$ = 6.33(3) and 6.14(1), where the standard deviation in last significant digits is in parentheses. Goodness-of-fit tests for various regression diagnostics enable the reliability of the parameter estimates to be determined. Most indices always predict the correct number of components when the SER is still much higher than 10. The Wernimont-Kankare procedure in INDICES performs a reliable determination of the instrumental standard deviation of spectrophotometer used $s_{inst}(A)$, predicts the number of light-absorbing components present n_c, and can also solve an ill-defined problem with severe collinearity in the spectra or very small changes in spectra.

AUTHOR INFORMATION

Corresponding Author

*Milan Meloun. Tel.: +420466037026. Fax: +420 466037068. E-mail: milan.meloun@upce.cz.

Funding Sources

The financial support of the Grant Agency IGA MZ ČR (Grant No. NS9831-4/2008) and of the Czech Ministry of Education (Grant No. MSM0021627502) is gratefully acknowledged.

REFERENCES

(1) Wikipedia; www.wikipedia.org/ (2010).
(2) Gear, R. W.; Miaskowski, C.; Gordon, N. C.; Paul, S. M.; Heller, P. H.; Levine, J. D. The kappa opioid nalbuphine produces gender- and dose-dependent analgesia and antianalgesia in patients with postoperative pain. *Pain* **1999**, *83*, 339–345.
(3) Barash, P. G. *Clinical anesthesia*, 6th ed.; Wolters Kluwer/Lippincott Williams & Wilkins: Philadelphia, PA, 2009; p xviii.
(4) Riviere, J. E.; Papich, M. G. *Veterinary pharmacology and therapeutics*, 9th ed.; Wiley-Blackwell: Ames, IA, 2008.
(5) Medicinenet; www.medicinenet.com/zolpidem/article.htm (2010).
(6) Lemmer, B. The sleep-wake cycle and sleeping pills. *Physiol. Behav.* **2007**, *90*, 285–293.
(7) Patat, A.; Naef, M. M.; Vangessel, E.; Forster, A.; Dubruc, C.; Rosenzweig, P. Flumazenil Antagonizes the Central Effects of Zolpidem, an Imidazopyridine Hypnotic. *Clin. Pharmacol. Ther.* **1994**, *56*, 430–436.
(8) Wesensten, N. J.; Balkin, T. J.; Davis, H. Q.; Belenky, G. L. Reversal of Triazolam-Induced and Zolpidem-Induced Memory Impairment by Flumazenil. *Psychopharmacology* **1995**, *121*, 242–249.
(9) Salva, P.; Costa, J. Clinical Pharmacokinetics and Pharmacodynamics of Zolpidem - Therapeutic Implications. *Clin. Pharmacokinet.* **1995**, *29*, 142–153.
(10) Noguchi, H.; Kitazumi, K.; Mori, M.; Shiba, T. Electroencephalographic properties of zaleplon, a non-benzodiazepine sedative/hypnotic, in rats. *J. Pharmacol. Sci.* **2004**, *94*, 246–251.
(11) Gulyás, Z.; Pöcze, G.; Petz, A.; Darvas, F. Pallas cluster—a new solution to accelerate the high-throughut ADME-TOX prediction. ComGenex-*CompuDrug, PKALC/PALLAS 2.1*; CompuDrug Chemistry Ltd., http://www.compudrug.com.
(12) Hillal, S. H.; Karickhoff, S. W.; Carriera, L. A. *Prediction of chemical reactivity parameters and physical properties of organic compound from molecular structure using SPARC*; Office of Research and Development, U.S. Enviromental Protection Agency, NC 27711: Washington, DC, March 2003.
(13) Leggett, D. J., Ed. *Computational Methods for the Determination of Formation Constants*; Plenum Press: New York, 1985.
(14) Havel, J.; Meloun, M. *Computational Methods for the Determination of Formation Constants*; Leggett, D. J., Ed.; Plenum Press: New York, 1985.
(15) Meloun, M.; Javůrek, M.; Havel, J. Multiparametric Curve Fitting. 10. A Structural Classification of Programs for Analyzing Multicomponent Spectra and Their Use in Equilibrium-Model Determination. *Talanta* **1986**, *33*, 513–524.
(16) Leggett, D. J.; McBryde, W. A. E. General Computer-Program for Computation of Stability-Constants from Absorbance Data. *Anal. Chem.* **1975**, *47*, 1065–1070.

(17) Leggett, D. J. Numerical-Analysis of Multicomponent Spectra. *Anal. Chem.* **1977**, *49*, 276–281.
(18) Leggett, D. J.; Kelly, S. L.; Shiue, L. R.; Wu, Y. T.; Chang, D.; Kadish, K. M. A Computational Approach to the Spectrophotometric Determination of Stability-Constants. 2. Application to Metalloporphyrin Axial Ligand Interactions in Non-Aqueous Solvents. *Talanta* **1983**, *30*, 579–586.
(19) Kankare, J. J. Computation of Equilibrium Constants for Multicomponent Systems from Spectrophotometric Data. *Anal. Chem.* **1970**, *42*, 1322–1326.
(20) Gans, P.; Sabatini, A.; Vacca, A. Investigation of equilibria in solution. Determination of equilibrium constants with the HYPERQUAD suite of programs. *Talanta* **1996**, *43*, 1739–1753.
(21) Gampp, H.; Maeder, M.; Meyer, C. J.; Zuberbuhler, A. D. Calculation of equilibrium constants from multiwavelength spectroscopic data-I. Mathematical considerations. *Talanta* **1985**, *32*, 95–101.
(22) Gampp, H.; Maeder, M.; Meyer, C. J.; Zuberbuhler, A. D. Calculation of equilibrium constants from multiwavelength spectroscopic data-II. SPECFIT: Two user-friendly programs in basic and standard fortran 77. *Talanta* **1985**, *32*, 251–64.
(23) Gampp, H.; Maeder, M.; Meyer, C. J.; Zuberbuhler, A. D. Calculation of equilibrium constants from multiwavelength spectroscopic data-III Model-free analysis of spectrophotometric and ESR titrations. *Talanta* **1985**, *32*, 1133–9.
(24) Gampp, H.; Maeder, M.; Meyer, C. J.; Zuberbuhler, A. D. Calculation of equilibrium constants from multiwavelength spectroscopic data-IV Model-free least-squares refinement by use of evolving factor analysis. *Talanta* **1986**, *33*, 943–51.
(25) Meloun, M.; Syrový, T.; Vrána, A. The thermodynamic dissociation constants of ambroxol, antazoline, naphazoline, oxymetazoline and ranitidine by the regression analysis of spectrophotometric data. *Talanta* **2004**, *62*, 511–22.
(26) Meloun, M.; Syrový, T.; Vrána, A. The thermodynamic dissociation constants of losartan, paracetamol, phenylephrine and quinine by the regression analysis of spectrophotometric data. *Anal. Chim. Acta* **2005**, *533*, 97–110.
(27) Meloun, M.; Syrový, T.; Vrána, A. The thermodynamic dissociation constants of haemanthamine, lisuride, metergoline and nicergoline by the regression analysis of spectrophotometric data. *Anal. Chim. Acta* **2005**, *543*, 254–266.
(28) Meloun, M.; Javůrek, M.; Militký, J. Computer Estimation of Dissociation-Constants 0.5. Regression-Analysis of Extended Debye-Huckel Law. *Mikrochim. Acta* **1992**, *109*, 221–231.
(29) *SPECFIT/32*; Spectrum Software Associates: Marlborough, MA, 2004.
(30) Meloun, M.; Bordovská, S.; Syrový, T.; Vrána, A. Tutorial on a chemical model building by least-squares non-linear regression of multiwavelength spectrophotometric pH-titration data. *Anal. Chim. Acta* **2006**, *580*, 107–121.
(31) Meloun, M.; Pluhařová, M. Thermodynamic dissociation constants of codeine, ethylmorphine and homatropine by regression analysis of potentiometric titration data. *Anal. Chim. Acta* **2000**, *416*, 55–68.
(32) Meloun, M.; Militký, J.; Forina, M. *Chemometrics for analytical chemistry, Vol. 1: PC-Aided Statistical Data Analysis*; Ellis Horwood: Chichester, 1992; p 330.
(33) Meloun, M.; Militký, J.; Forina, M. *Chemometrics for analytical chemistry, Vol. 2: PC-Aided Regression and Related Methods*; Ellis Horwood: Chichester, 1994; p 400.
(34) Meloun, M.; Syrový, T.; Vrána, A. Determination of the number of light-absorbing species in the protonation equilibra of selected drugs. *Anal. Chim. Acta* **2003**, *489*, 137–151.
(35) Meloun, M.; Čapek, J.; Mikšík, P.; Brereton, R. G. Critical comparison of methods predicting the number of components in spectroscopic data. *Anal. Chim. Acta* **2000**, *423*, 51–68.
(36) Meloun, M.; Havel, J.; Högfeldt, E. *Computation of solution equilibria: a guide to methods in potentiometry, extraction, and spectrophotometry*; Ellis Horwood: Chichester, England, 1988; p x.
(37) *MARVIN*; http://www.chemaxon.com/conf/Prediction_of_dissociation_constant_using_microcon-stants.pdf and http://www.chemaxon.com/conf/New_method_for_pKa_estimation.pdf.
(38) Meloun, M.; Bordovská, S.; Kupka, K. Outliers detection in the statistical accuracy test of a pK(a) prediction. *J. Math. Chem.* **2010**, *47*, 891–909.
(39) *ORIGIN8*; OriginLab Corporation: Northampton, MA, 2010.
(40) Dornette, W. H. L. *Clinical care*; F. A. Davis: Philadelphia, PA, 1967; p 153.
(41) *ADSTAT 1.25, 2.0, 3.0 (Windows 95)*; TriloByte Statistical Software Ltd.: Pardubice, Czech Republic, 2010.